



# Differentially Expressed Genes Analysis of Brown Adipose Tissue During Cold Acclimation in Male Tree Shrews (*Tupaia belangeri*) based on RNA-Seq

Dong-Min Hou<sup>1</sup>, Ting Jia<sup>2</sup>, Hui-Juan Wang<sup>1</sup>, Zheng-Kun Wang<sup>1</sup> and Wan-Long Zhu<sup>1\*</sup>

<sup>1</sup>Key Laboratory of Ecological Adaptive Evolution and Conservation on Animals-Plants in Southwest Mountain Ecosystem of Yunnan, School of Life Sciences, Yunnan Normal University, 1<sup>st</sup> Yuhua District, Chenggong County, Kunming City, Yunnan Province, Kunming, 650500, China

<sup>2</sup>Yunnan University of Business Management, Kunming, 650106, China

## ABSTRACT

Thermogenic function of brown adipose tissue (BAT) was known to be markedly elevated when animals were exposed to the cold. In the present study, transcriptome sequencing of BAT in *Tupaia belangeri* between control and cold acclimation group were carried out by Illumina novaseq 6000 platform. Then the pathways and key genes related to lipid metabolism and energy metabolism were screened out by bioinformatics analysis. The results showed that there were significant differences in the expression of 2879 genes in cold acclimation group compared with that of control group, 1181 were up-regulated and 1698 were down-regulated in cold acclimation group. Pathway analyses showed that the differentially expressed genes were significantly enriched in oxidative phosphorylation, steroid biosynthesis, glycerophospholipid and fatty acid metabolism pathways related to energy metabolism and lipid metabolism. Differentially expressed genes *ND3*, *ND4*, *ND5*, *ND6*, *ND4L*, *CYTB*, *ATP8* and *ATP6* in oxidative phosphorylation pathway were significantly up-regulated. Key genes related to lipid metabolism were identified as *ELOVL6*, *ACACA*, *HSD17B12*, *SQLE*, *LSS*, *DHCR7*, *DHCR24*, *CYP51A1*, *HMGCS1*, *LPL*, and *ACACA*, etc, which were down-regulated in the lipid metabolism pathway. All of the above results indicated that *T. belangeri* could adapt to the cold environment by regulating genes expression in oxidative phosphorylation, steroid biosynthesis, glycerophospholipid and fatty acid metabolism pathways in BAT. Among them, expressions of genes in oxidative phosphorylation pathway were up-regulated, and most of the genes related to the lipid metabolism pathway were down-regulated, which promoted energy expenditure and thermogenesis.

## Article Information

Received 10 December 2021

Revised 05 January 2022

Accepted 30 January 2022

Available online 09 May 2022 (early access)

## Authors' Contribution

D-MH, H-JW and TJ carried out the experiment. W-LZ and Z-KW conceived and the study coordinated and drafted the manuscript. All authors read and approved the final manuscript.

## Key words

*Tupaia belangeri*, Transcriptome, Brown adipose tissue, Cold acclimatization, Non-shivering thermogenesis, Genes related to lipid metabolism, Genes of oxidative phosphorylation pathway

## INTRODUCTION

Cold exposure imposes a metabolic challenge to mammals that must be met by the response of animals' body tissues to ensure homeothermy. Brown adipose tissue (BAT) was the main site of cold-induced non-shivering thermogenesis (NST) (Klingenspor, 2003), which has the remarkable ability to dissipate excess energy as heat in a

process known as adaptive thermogenesis. Transcriptome sequencing technology, as the main method of studying transcriptomics, has high sensitivity in transcript identification and the quantification of gene expression (Conesa *et al.*, 2016). Researchers used transcriptome sequencing technology to analysis the differences of BAT and white adipose tissue (WAT) in mice under cold exposure, the results indicated that the effects of cold exposure on the gene expression profiles of BAT were much greater than those of WAT (Watanabe *et al.*, 2011). Other study have shown that expression of genes related to lipid metabolism and oxidative phosphorylation pathways in BAT of mice or rats significantly changed under cold exposure (Shore *et al.*, 2013; Rosell *et al.*, 2014).

Tree shrew, *Tupaia belangeri* (Mammalia: Scandentia: Tupaiidae), a squirrel-like lower primate, is a unique Oriental species. This animal originates from the tropical

\* Corresponding author: [zwl\\_8307@163.com](mailto:zwl_8307@163.com)  
0030-9923/2022/0001-0001 \$ 9.00/0



Copyright 2022 by the authors. Licensee Zoological Society of Pakistan.

This article is an open access article distributed under the terms and conditions of the Creative Commons Attribution (CC BY) license (<https://creativecommons.org/licenses/by/4.0/>).

island, in China; and is mainly distributed in Yunnan, Guizhou and Sichuan (Bremer *et al.*, 2011). Judging from the distribution characteristics of existing tree shrews, the Yunnan-Kweichow Plateau and the southeastern part of the Qinghai-Tibet Plateau, that is, parts of the Hengduan Mountains may constitute the northern limit of the distribution of *T. belangeri*, and low temperature may limit its northward spread. Our group previously used classic physiological research methods to confirm that cold acclimation increased the BAT mass, uncoupling protein 1 (UCP1) content, and NST in *T. belangeri* to maintain body temperature, but the proportion of NST in the total heat production showed a gradual decline (Zhang *et al.*, 2017). In the present study, we used RNA-seq to analyze the differential expression of genes in BAT of *T. belangeri* under cold acclimation, providing relevant information such as genes function and enrichment, and realizing the analysis of the function of thermogenesis genes and pathways, thus providing important reference for the study of the mechanism of cold adaptation heat-producing in small mammals.

## MATERIALS AND METHODS

### Animals

*T. belangeri* were captured (25°25'-26°22'N, 102°13'-102°57'E, at 1679 m altitude) at the boscaje of Luquan County, Yunnan Province, and maintained at the School of Life Sciences, Yunnan Normal University, Kunming (1910 m altitude). Average body mass of all animals was 115.36±3.65g, after one month of adaptation at room temperature; the animals were divided into 2 groups according to their body mass, with 6 male individuals in each group: One group was kept at 25°C±1°C for 28 days; these animals comprised the control group. A second group was kept at 5°C±1°C for 28 days comprised the cold acclimatized group. Two groups were healthy adults, and housed individually in a wire cage (40 cm×40 cm×40 cm), The cage environment was maintained at 12L:12D (lights on at 08:00), and 65–92% relative humidity. Water and foods were provided *ad libitum*. *T. belangeri* were fed a food mixture containing 30% corn flour, 20% wheat flour, 5% fish meal, 6% wheat bran, 3.6% milk powder, 10% sugar, 2% yeast, 3% electrolytic multivitamin, 0.4% edible salt, and 20% eggs, as well as apples, pears and other fruits twice weekly. After 28 days of acclimatization and testing, all animals were anesthetized with ether and then killed. Samples of BAT was taken from each animal and immediately frozen in liquid nitrogen followed by storage at -80°C prior to analysis.

### Total RNA extraction and RNA-Seq preparation

Total RNA was extracted from BAT according to

miRNeasy Mini Kit instructions. The integrity, purity and concentration of total RNA were confirmed using a Bioanalyzer 2100 (Agilent Technologies). The total RNA content > 3µg, and the integrity (RIN) > 7.0 was qualified, which can be used in the next experiment. cDNA synthesis was done using TruSeq PE Cluster Kit v4-cBot-HS (Illumina). RNA-seq libraries were constructed according to the manufacturer's instructions and sequenced using the Illumina novaseq 6000 platform.

### RNA-Seq data analysis

Raw data (raw reads) of fastq format were firstly processed through in-house perl scripts. In this step, clean data (clean reads) were obtained by removing reads containing adapter, reads containing ploy-N and low quality reads from raw data. At the same time, Q20, Q30, GC content and clean data were calculated. All the downstream analyses were based on clean data with high quality. These clean reads were then mapped to the tree shrew reference genome sequence (version tupBell1). Hisat2 tools soft were used to map with reference genome. Quantification of gene expression levels were estimated by fragments per kilobase of transcript per million fragments mapped. The formula is shown as follow:

$$\text{FPKM} = \frac{\text{cDNA Fragments}}{\text{mapped fragments (millions)} \times \text{transcript length (kb)}}$$

Through PCA principal component analysis of two groups of data under different conditions, the difference and distance between groups were reflected on the coordinate axis. Differential expression analyses of two groups were performed using the DEseq. The screening criteria were fold change (FC) ≥ 2 and false discovery rate (FDR) < 0.01 (Shore *et al.*, 2013), and count of differentially expressed genes (DEGs) of log<sub>2</sub> FC >4. Functional enrichment analysis was performed with KOBAS using pathways related to metabolism from the KEGG database annotation (Mao *et al.*, 2005). The significant enrichment Q-value (Q-value is the P-value corrected for multiple hypothesis testing) was calculated to identify the pathways with significant enrichment, and key genes were screened based on FPKM values and related literature reports.

### Quantitative real time PCR

To verify the reliability of transcriptome sequencing results, 8 DEGs were selected for RT-PCR quantification (Table 1), and the reference gene primer sequence was

F: GAGAGGGAAATCGTGCGTGAC

R: CATCTGCTGGAAGGTGGACA

The design of DEGs primer and the steps of real-time quantitative operation are detailed Zhang *et al.* (2017).

**Table I. Primers of real-time quantitative PCR.**

Gene name	Gene ID	Up or down regulation in 28d group	Primers 5'→3'
<i>UCP1</i>	ENSTBEG00000000042	up	F: CGGAATTCCAGCCAAGATGGTGAGT R: CGGAATTCGTAGGTCCCAGTGTAGCG
<i>UCP2</i>	ENSTBEG00000001484	up	F: TCTACAATGAGCTGCGTGTG R: GGTCAGGATCTTCATGAGGT
<i>CYTB</i>	ENSTBEG000000021344	up	F: GGATCTGACCAAGACCTGTGAC R: TCCCTCCGTTTCTGGTTTAC
<i>PRDM16</i>	ENSTBEG000000009948	down	F: CTGTACACAGCCTGGAGCAGCACAT R: GGTAGGGTGTCTGTGCACGTTACC
<i>LPL</i>	ENSTBEG000000015298	down	F: AGCGGGAGCCTGACTCTAAC R: GAGCGTTCGTGGGAGCATT
<i>ACACA</i>	ENSTBEG000000008501	down	F: TTGTTTGGTCGTGACTGCTC R: TTTGGCAAGTTTCACTGCAC
<i>AKT2</i>	ENSTBEG000000001484	down	F: GCCACGACCAACACCT R: TAGCCCGCATCCACTC
<i>SLC2A4</i>	ENSTBEG000000000866	down	F: AACTGGACCTGTAACCTCA R: AGGAGGACGGCAAAT

**Table II. Statistical of each sample output data.**

Sample	Clean reads (pair end reads)	Clean bases	GC content (%)	%≥ Q30
Control group	1 24271981	7275479188	50.55	93.62
	2 23753571	7115963640	51.24	93.71
	3 24884956	7454768158	51.22	93.84
	4 24024588	7198789296	50.32	93.68
	5 23755489	7118049154	51.38	93.93
	6 25652547	7685405490	51.00	94.15
Cold acclimatization group	1 19329643	5737840076	46.24	94.45
	2 21927532	6534981438	46.55	94.03
	3 22038282	6549278676	45.32	94.33
	4 24124587	7178623100	43.92	94.72
	5 22246352	6614415322	45.76	94.74
	6 21715515	6469509798	44.86	94.67

## RESULTS

### Transcriptome data evaluation

All samples were qualified (total RNA content > 3 µg, RIN ≥ 7). The proportion of clean data of all samples with Q30 was more than 93.62%, and the GC content were about 50%, the quality of the data obtained by sequencing was reliable (Table II). The results of principal component analysis showed that the data composition of the two groups was significantly different, the samples in

the groups were clustered, and the obtained results were consistent with the expected results (Fig. 1).

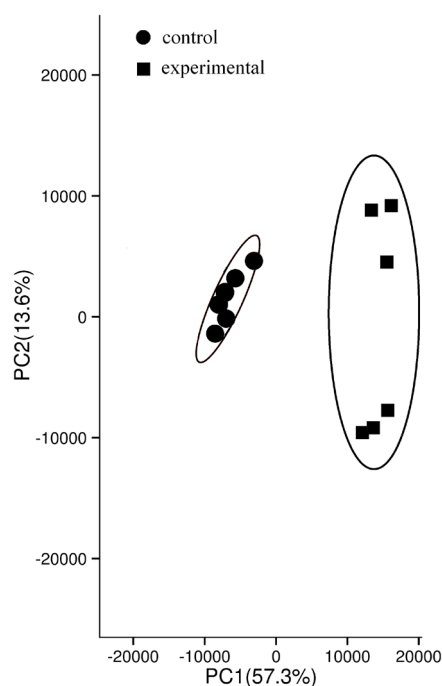


Fig. 1. PCA principal component analysis diagram. Note: Points with different colors or shapes represent sample groups under different environments or conditions. The scales of horizontal and vertical coordinates are relative distances, which have no practical significance.

*Bioinformatics analysis*

Using a significance level of  $FDR < 0.05$ ,  $FC \geq 2$ , we found a total of 2,879 DEGs, of which 1,181 and 1,698 genes showed increased and reduced expression under 28-day cold exposure, respectively. Notably, the *UCP1* ( $\log_2FC=1.316063$ ) gene encoding UCP1 reported previously as having increased expression in BAT after cold exposure. The present study (Tables III) showed that the expression of 28 genes were significantly up- or down-regulated more than four folds by cold exposure, these include *ATP8*, *ATP6*, *ND3*, *ND4L*, *ND4*, *ND5* and *CYT6* genes in oxidative phosphorylation pathway, as well as *ACACA*, *ELOVL6* and *HSD17B12* genes that played an inhibitory role in fatty acid metabolism, and so on. Functional enrichment analyses of the genes with

the most pronounced cold-induced expression using Kyoto Encyclopedia of Genes and Genomes (KEGG) pathways revealed a significant enrichment of metabolic pathways, including oxidative phosphorylation, steroid biosynthesis, fatty acid metabolism, glycerophospholipid metabolism (Fig. 2). The most highly enriched pathway for up-regulated genes were oxidative phosphorylation pathway, which includes several genes encoding NADH dehydrogenase (*ND3*, *ND4*, *ND5*, *ND6* and *ND4L*), cytochrome c reductase (*CYT6*) and ATP synthase (*ATP6*, *ATP8*). Most genes related to lipid metabolism pathway were repressed in BAT, including *SQLE*, *LSS*, *DHCR24*, *DHCR7*, *CYP51A1*, *SCD*, *ACSL4*, *ELOVL6*, *ACACA*, *HSD17B12*, *GPD2*, *LPGAT1*, and *SELENOI* (Table IV).

**Table III. Most differentially expressed genes.**

Gene ID	Gene name	$\log_2FC$	up/down
ENSTBEG00000021330	<i>ATP8</i>	7.936743241	up
ENSTBEG00000021331	<i>ATP6</i>	4.953971529	up
ENSTBEG00000021334	<i>ND3</i>	6.545693211	up
ENSTBEG00000021336	<i>ND4L</i>	5.016029694	up
ENSTBEG00000021337	<i>ND4</i>	6.017905995	up
ENSTBEG00000021341	<i>ND5</i>	4.263457202	up
ENSTBEG00000021344	<i>CYT6</i>	4.413630364	up
ENSTBEG00000004145	<i>ELOVL6</i>	-4.094294687	down
ENSTBEG00000008501	<i>ACACA</i>	-4.208078151	down
ENSTBEG00000016576	<i>HSD17B12</i>	-4.154425257	down
ENSTBEG00000003366	<i>ZMYND10</i>	4.014191841	up
ENSTBEG00000007999	<i>LRRC34</i>	4.671748042	up
ENSTBEG00000005473	<i>ARL14</i>	4.672650726	up
ENSTBEG00000010081	<i>EPGN</i>	4.122101729	up
ENSTBEG00000005549	<i>ASGR2</i>	4.174722567	up
ENSTBEG00000014737	<i>EMP1</i>	-4.707252838	down
ENSTBEG00000001606	<i>CDC42EP3</i>	-4.774003734	down
ENSTBEG00000003839	<i>PLEKHF1</i>	-4.251165321	down
ENSTBEG00000004403	<i>DUSP14</i>	-5.196061636	down
ENSTBEG00000005559	<i>ZDHHC23</i>	-4.769844094	down
ENSTBEG00000005948	<i>ZFP36</i>	-6.377754145	down
ENSTBEG00000010112	ENSTBEG00000010112	4.141663745	up
ENSTBEG00000012297	ENSTBEG00000012297	4.911709954	up
ENSTBEG00000001950	ENSTBEG00000001950	4.079109484	up
ENSTBEG00000013693	ENSTBEG00000013693	4.402327939	up
ENSTBEG00000017771	ENSTBEG00000017771	4.134596289	up
ENSTBEG00000007362	ENSTBEG00000007362	-4.547748676	down
ENSTBEG00000001052	ENSTBEG00000001052	-4.163123945	down

**Table IV. KEGG significantly enriched pathway list of up regulated and down regulated key genes.**

Gene ID	Gene name	log <sub>2</sub> FC	up/ down
<b>Oxidative phosphorylation</b>			
ENSTBEG00000021334	<i>ND3</i>	6.545693211	up
ENSTBEG00000021337	<i>ND4</i>	6.017905995	up
ENSTBEG00000021341	<i>ND5</i>	4.263457202	up
ENSTBEG00000021336	<i>ND4L</i>	5.016029694	up
ENSTBEG00000021342	<i>ND6</i>	3.206990989	up
ENSTBEG00000021344	<i>CYTB</i>	4.413630364	up
ENSTBEG00000021330	<i>ATP8</i>	7.936743241	up
ENSTBEG00000021331	<i>ATP6</i>	4.953971529	up
<b>Steroid biosynthesis</b>			
ENSTBEG00000000773	<i>CYP51A1</i>	-3.452344132	down
ENSTBEG00000003064	<i>SQLE</i>	-1.919891924	down
ENSTBEG00000007270	<i>DHCR24</i>	-3.877599142	down
ENSTBEG00000013059	<i>DHCR7</i>	-2.100319058	down
ENSTBEG00000016213	<i>LSS</i>	-2.106663039	down
<b>Fatty acid metabolism</b>			
ENSTBEG00000000654	<i>SCD</i>	-2.913797823	down
ENSTBEG00000002831	<i>ACSL4</i>	-2.253983817	down
ENSTBEG00000004145	<i>ELOVL6</i>	-4.094294687	down
ENSTBEG00000008501	<i>ACACA</i>	-4.208078151	down
ENSTBEG00000016576	<i>HSD17B12</i>	-4.154425257	down
<b>Glycerophospholipid metabolism</b>			
ENSTBEG00000014623	<i>GPD2</i>	-3.515187858	down
ENSTBEG00000013545	<i>LPGATI</i>	-2.243027443	down
ENSTBEG00000016576	<i>SELENOI</i>	-2.795006506	down

This study verified 8 DEGs. The comparison results of Real-time PCR and RNA-Seq were showed in Figure 3. The up and down regulation trends of gene expression between the two results were consistent, indicating that the quality of transcriptome sequencing was reliable.

## DISCUSSION

Small mammals in the wild maintain body temperature by increasing thermogenesis when they are exposed to low temperatures (Wang and Wang, 1990). Studies showed that there were significant differences in gene expression in BAT of yak between cold and warm seasons (Zhu *et al.*, 2021). In the present study, it was found that 2879 genes were up-regulated or down-regulated in the cold acclimation group, suggesting that *T. belangeri* may adapt to the cold

environment by changing the expression pattern of genes. Studies suggested that UCP1 was the main substance that determines the heat production of BAT (Mei *et al.*, 2019). In our study, expression level of heat-producing gene *UCP1* increased after cold acclimation, which was consistent with the results of previous studies, but the up-regulated multiple was not significant ( $\log_2FC = 1.3$ ), indicating the reason why the proportion of NST in total heat-producing decreased gradually (Zhang *et al.*, 2017). In the KEGG enrichment analysis of this study, DEGs were significantly enriched in oxidative phosphorylation related to energy metabolism, steroid biosynthesis, fatty acid metabolism, and glycerolipid metabolism pathways related to lipid metabolism, suggesting that lipid metabolism pathways in *T. belangeri* may play an important role in the mechanism of cold adaptation. Previous analysis of transcriptome pathways showed that the genes most significantly induced in mouse BAT under cold exposure were those involved in glycerophospholipid synthesis and fatty acid elongation (Rosell *et al.*, 2014).

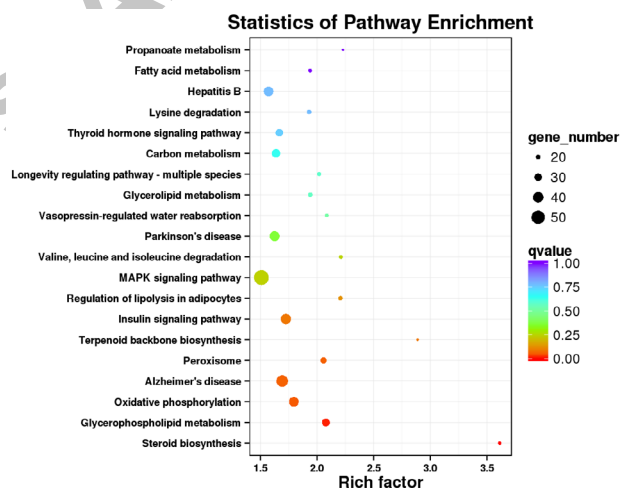


Fig. 2. KEGG pathway enrichment bubble diagram of differentially expressed genes.

Mitochondrial protein-coding genes played a major role in the oxidative phosphorylation system (Leonard and Schapira, 2000), and the four enzymes encoded by them were the driving force for ATP synthesis. Studies showed that after long-term cold exposure in mice, gene expression in BAT showed significant changes, and the oxidative phosphorylation pathway was significantly up-regulated in BAT (Rosell *et al.*, 2014). In present study, compared with the control group, mitochondrial protein-coding genes NADH Dehydrogenase subunit 3 (*ND3*), NADH dehydrogenase subunit 4 (*ND4*), NADH dehydrogenase subunit 5 (*ND5*), NADH dehydrogenase subunit 6 (*ND6*),

NADH dehydrogenase subunit 4L (*ND4L*), cytochrome b (*CYTB*), ATP synthase F0 subunit 6 (*ATP6*) and ATP synthase F0 subunit 8 (*ATP8*) were highly expressed in the oxidative phosphorylation pathway of BAT in the cold acclimatization group, all of which were unregulated by more than 4 fold. These results indicated that the synthesis of ATP was promoted in the response to cold environment, which provided more energy for animals. Studies have shown that mitochondrial protein-encoding genes defects could lead to increased mitochondrial damage and decreased function, which ultimately led to a decrease in the ability of oxidative phosphorylation (Luoma *et al.*, 2015). NADH dehydrogenase encoded by *ND3*, *ND4*, *ND5*, *ND6* and *ND4L* was one of the largest membrane-bound enzymes in cells. Studies have shown that the variation of *ND3* could cause a loss of the role of mitochondrial oxidative phosphorylation. If the mitochondrial oxidative energy supply was increased, it might cause the expression level of *ND3* to also increase (Hinokio *et al.*, 1995; Wang *et al.*, 2013). In this study, *ND3* was up-regulated 6 folds, suggesting that *T. belangeri* under cold acclimation may promote mitochondrial oxidative energy supply through the regulation of this gene. Inhibition of protein synthesis, transcription, and ion transport can lead to inhibition of energy expenditure. Among the 13 protein-coding genes, the structure and function of *CYTB* gene has been most thoroughly studied, it was an important mediator of electron transfer in oxidative phosphorylation, and could conduct transcription and protein synthesis in mitochondria itself (Schoepp *et al.*, 2000). Therefore, our data demonstrate that *T. belangeri* might adapt to the cold environment by the regulation of this gene to maximize energy expenditure. *ATP6/8* of the genes encoding ATP synthase protein 6/8. Studies have shown that the expression of *ATP6/8* in BAT during hibernation in black-line hamsters is also up-regulated by 4 folds. If the expression of *ATP6* gene was down-regulated, ATP production can reduce, thereby affecting energy metabolism (Hittel *et al.*, 2013).

Lipid was the main component of biofilm and important structure of organism. It not only participates in energy supply and storage of organism, but also can be transformed into various derivatives to participate in metabolic activities. Studies have performed transcriptome analysis of BAT in mice under cold exposure; they proposed the response to cold stress involves decreased gene expression in a range of lipid metabolism in order to maximize pathways involved in heat production (Shore *et al.*, 2013). Our data demonstrate that the general trend was for a reduction in the expression of a large number of genes involved in steroid biosynthesis, glycerophospholipid and fatty acid metabolism pathways related to lipid metabolism, and far fewer genes were up-regulated by

the cold challenge. This might represent a mechanism for reducing metabolic reactions so that metabolism could be focused on the cell thermogenic functions, particularly in BAT, that are essential to prevent hypothermia.

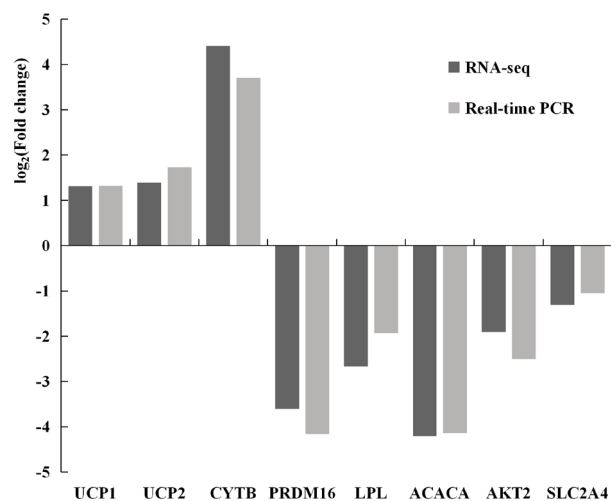


Fig. 3. Comparison of the RNA-Seq and Real-time PCR results.

Steroids were mainly composed of cholesterol. Studies have shown that insufficient cholesterol content could cause more free fatty acid (FFA) to remain in the circulatory system of mice to provide energy sources for other tissues and organs of the animal body (Dugail *et al.*, 2003). In our study, compared with the control group, the squalene epoxidase (*SQLE*), lanosterol synthase (*LSS*), 24-dehydrocholesterol reductase (*DHCR24*), 7-dehydrocholesterol reductase (*DHCR7*), and lanosterol synthase (*LSS*) genes encoding proteins related to cholesterol synthesis were significantly down-regulated in the cold acclimation group. These results suggested that *T. belangeri* might reduce the synthesis of cholesterol in BAT by down-regulating *SQLE*, *LSS*, *DHCR24*, *DHCR7*, and *CYP51A1* in cold environments, which left more FFA in the circulatory system to provide energy source for other tissues and organs of animal body. *SQLE* and *LSS* were located in the endoplasmic reticulum, and squalene epoxidase encoded by *SQLE* was one of the key rate-limiting enzymes that catalyze the conversion of squalene to squalene 2, 3-epoxides in cholesterol biosynthesis. Studies have shown that inhibition of *SQLE* could effectively reduce cholesterol synthesis (Ferdinandusse *et al.*, 2017). *LSS* was a member of the gene super family OSC (3S-2,3 epoxy-squalene cyclase), and the production of lanosterol catalyzed by *LSS* was a key step in the synthesis of sterols in animals. *CYP51* was one of the most

widely distributed members of the CYP superfamily of cytochromases. The *CYP51A1* gene encoding this enzyme originated from prokaryotes and was widely distributed in eukaryotes (Lepesheva and Waterman, 2011).

Glycerophospholipid were the most abundant phospholipids in animals. The metabolism of each phospholipid formed a complex network and was regulated by a variety of metabolic enzymes (Liu and Huang, 2013). Fatty acid metabolism mainly includes *de novo* synthesis, oxidation, desaturation and lengthening of fatty acids (FA) to produce FA with different saturation degrees and different carbon chain lengths. In our study, compared with a control group, stearoyl-CoA desaturase (*SCD*), acyl-CoA synthetase long-chain family member 4 (*ACSL4*), ELOVL fatty acid elongase 6 (*ELOVL6*), acetyl-CoA carboxylase alpha (*ACACA*) and hydroxysteroid 17-beta dehydrogenase 1 (*HSD17B12*) genes related to fatty acid metabolism and glycerol-3-phosphate dehydrogenase 2 (*GPD2*), lysophosphatidylglycerol acyltransferase 1 (*LPGATI*) and selenoprotein I (*SELENOI*) involved in the glycerophospholipid metabolism pathway were significantly down-regulated in cold acclimation group. This result was consistent with previous studies that showed significant changes in genes involved in glycerophospholipid synthesis and fatty acid extension in BAT of cold-stimulated mice (Marcher *et al.*, 2015). Among them, *ACACA* was a target gene of steroid response element binding protein-1 (SREBP-1), and the enzyme encoded by it was a key rate-limiting enzyme regulating *de novo* synthesis of fatty acids. Its expression was also regulated by a variety of hormones. Studies have shown that the down-regulation of the *ACACA* gene expression led to a decrease in fatty acid *de novo* synthesis (Knobloch *et al.*, 2013; Bakhtiarizadeh and Alamouti, 2020). *ACSL4* belonged to the long-chain family of acyl-CoA synthase, which mainly catalyzed the activation of long-chain fatty acids to synthesize cell lipids. Down-regulation of *ACSL4* reduced the intracellular triglyceride concentration (Fan *et al.*, 2020). *ELOVL6* belonged to the sixth member of the ultra-long-chain elongase gene family. It was an important rate-limiting enzyme for the extension and synthesis of long-chain fatty acids. Its main function in fatty acid metabolism was the extension of fatty acids above C16. Studies have shown that *ELOVL6* gene down regulation of expression inhibited the extension of C16:1 to C18:1 (Corominas *et al.*, 2013; Green *et al.*, 2010). Fatty acid desaturation index in fat cells of *ELOVL6* knockout mice decreased significantly, and the content of linoleic acid also decreased significantly (Sunaga *et al.*, 2013). 17 $\beta$ -SHD12 belonged to the short-chain dehydrogenase/reductase (SDR) superfamily and has been discovered

relatively late in humans (Peltoketo *et al.*, 1999), recently, it has been found that *HSD17B12* gene regulates fatty acid synthesis and the elongation of long-chain fatty acyl-CoA in fatty acid metabolism (Moon and Horton, 2003). *SCD* was a key enzyme that catalyzes the desaturation of saturated fatty acids. Studies have shown that over expression of *SCD* can easily lead to fat accumulation (Nagao *et al.*, 2019). The above results in present study suggested that *T. belangeri* may adapt to cold environment by down-regulating *SCD*, *ACSL4*, *ELOVL6*, *ACACA*, and *HSD17B12* genes to regulate fatty acid synthesis in BAT.

The *GPD2* gene encodes glycerol 3-phosphate dehydrogenase 2, which was the key enzyme linking glycolysis and oxidative phosphorylation, and its play an important role was as part of the glycerophosphate shuttle (Orr *et al.*, 2014). Studies have shown that the decreased activity of *GPD2* limited the gluconeogenesis of lactic acid and glycerol, and reduced endogenous glucose production, and could also inhibit the proliferation of tumor cells (Madiraju *et al.*, 2014). In our study, *GPD2* gene was significantly down-regulated, which could not only regulate energy balance, but also provided a target for disease treatment. As a remodeling enzyme, *LPGATI* could reconstitute lysophosphatidylglycerol into PG. Studies have found that the variation of *LPGATI* gene played an important role in the process of weight regulation (Traurig *et al.*, 2013). Selenoprotein I (*SELENOI*) was also known as ethanolaminephosphotransferase 1 (*EPT1*). Studies have shown that mutations in the *SELENOI* gene significantly reduced the activity of encoding *EPT1*, leading to impeded PE synthesis and increased ATP synthesis, which interfered with the metabolic pathway (Ahmed *et al.*, 2017; Ma *et al.*, 2021). In this study, *SELENOI* gene was down-regulated, indicating that PE synthesis in BAT of *T. belangeri* was reduced under cold acclimation, thus affecting energy metabolism of the animals.

We measured the adaptive changes of genes in BAT in *T. belangeri* under cold acclimation at the transcriptome level. In summary, cold acclimation induced a significant up-regulation of genes expression related to oxidative phosphorylation, and significant down-regulation of genes expression related to steroid biosynthesis, glycerophospholipid metabolism, and fatty acid metabolism, which ultimately promoted energy expenditure and heat production. In addition, we also found that the heat-producing gene *UCP1* was up-regulated after cold acclimation, but it was not significantly up-regulated, which might be the reason why the proportion of NST to total heat-producing decreased gradually in the process of cold acclimation and limited its northward spread the reason.

## ACKNOWLEDGMENTS

This research was financially supported by National Science Foundation of China (No. 32160254), Yunnan Ten Thousand Talents Plan Young & Elite Talents Project (YNWR-QNRC-2019-047) and Young and Middle-aged Academic and Technical Leaders Reserve Talents Project of Yunnan Province (2019HB013).

### Ethics statement

The protocol and study were approved by the Animal Care and Use Committee of the School of Life Sciences, Yunnan Normal University (No. 13-0901-011).

### Statement of conflict of interest

The authors have declared no conflict of interest.

## REFERENCES

- Ahmed, M.Y., Al-Khayat, A., Al-Murshedi, F., Al-Futaisi, A., Chioza, B.A., Fernandez-Murray, J.P., Self, J.E., Salter, C.G., Harlalka, G.V., Rawlins, L.E., Al-Zuhaibi, S., Al-Azri, F., Al-Rashdi, F., Cazenave-Gassiot, A., Wenk, M.R., Al-Salmi, F., Patton, M.A., Silver, D.L., Baple, E.L., McMaster, C.R. and Crosby, A.H., 2017. A mutation of *EPT1* (*SELENOI*) underlies a new disorder of Kennedy pathway phospholipid biosynthesis. *Brain*, **140**: 547-554. <https://doi.org/10.1093/brain/aww318>
- Bakhtiarzadeh, M.R. and Alamouti, A.A., 2020. RNA-Seq based genetic variant discovery provides new insights into controlling fat deposition in the tail of sheep. *Sci. Rep.*, **10**: 13525. <https://doi.org/10.1038/s41598-020-70527-8>
- Bremer, C.M., Sominskaya, I., Skrastina, D., Pumpens, P., Abd El-Wahed, A., Beutling, U., Frank, R., Fritz, H.J., Hunsmann, G., Gerlich, W.H. and Glebe, D., 2011. N-terminal myristoylation-dependent masking of neutralizing epitopes in the preS1 attachment site of hepatitis B virus. *J. Hepatol.*, **5**: 29-37. <https://doi.org/10.1016/j.jhep.2010.10.019>
- Conesa, A., Madrigal, P., Tarazona, S., Gomez-Cabrero, D., Cervera, A., McPherson, A., Szczesniak, M.W., Gaffney, D.J., Elo, L.L., Zhang, X.G. and Mortazavi, A., 2016. A survey of best practices for RNA-seq data analysis. *Genome Biol.*, **17**: 13. <https://doi.org/10.1186/s13059-016-0881-8>
- Corominas, J., Ramayo-Caldas, Y., Puig-Oliveras, A., Perez-Montarelo, D., Noguera, J.L., Folch, J.M. and Ballester, M., 2013. Polymorphism in the *ELOVL6* gene is associated with a major QTL effect on fatty acid composition in pigs. *PLoS One*, **8**: e53687. <https://doi.org/10.1371/journal.pone.0053687>
- Dugail, I., Le, Lay, S., Varret, M., Le Liepvre, X., Dagher, G. and Ferre, P., 2003. New insights into how adipocytes sense their triglyceride stores. Is cholesterol a signal? *Horm. Metab. Res.*, **35**: 204-210. <https://doi.org/10.1055/s-2003-39475>
- Fan, Y.L., Han, Z.Y., Lu, X.B., Zhang, H.M., Arbab, A.A.I., Loo, J.J., Yang, Y. and Yang, Z.P., 2020. Identification of milk fat metabolism-related pathways of the bovine mammary gland during mid and late lactation and functional verification of the *ACSL4* gene. *Genes*, **11**: 1357. <https://doi.org/10.3390/genes11111357>
- Ferdinandusse, S., Falkenberg, K.D., Koster, J., Mooyer, P.A., Jones, R., van Roermund, C.W.T., Pizzino, A., Schrader, M., Wanders, R.J.A., Vanderver, A. and Waterham, H.R., 2017. ACBD5 deficiency causes a defect in peroxisomal very long-chain fatty acid metabolism. *J. med. Genet.*, **54**: 330-337. <https://doi.org/10.1136/jmedgenet-2016-104132>
- Green, C.D., Ozguden-Akkoc, C.G., Wang, Y., Jump, D.B. and Olson, L.K., 2010. Role of fatty acid elongases in determination of de novo synthesized monounsaturated fatty acid species. *J. Lipid Res.*, **51**: 1871-1877. <https://doi.org/10.1194/jlr.M004747>
- Hinokio, Y., Suzuki, S., Komatu, K., Ohtomo, M., Onoda, M., Matsumoto, M., Hirai, S., Sato, Y., Akai, H., Abe, K., Miyabayasi, S., Abe, R. and Toyota, T., 1995. A new mitochondrial DNA deletion associated with diabetic amyotrophy, diabetic myoatrophy and diabetic fatty liver. *Muscle Nerv. Suppl.*, **3**: S142-S149. <https://doi.org/10.1002/mus.880181428>
- Hittel, D.S. and Storey, K.B., 2002. Differential expression of mitochondria-encoded genes in a hibernating mammal. *J. exp. Biol.*, **205**: 1625-1631. <https://doi.org/10.1242/jeb.205.11.1625>
- Klingenspor, M., 2003. Cold-induced recruitment of brown adipose tissue thermogenesis. *Exp. Physiol.*, **88**: 141-148. <https://doi.org/10.1113/eph8802508>
- Knobloch, M., Braun, S.M.G., Zurkirchen, L., von Schoultz, C., Zamboni, N., Arauzo-Bravo, M.J., Kovacs, W.J., Karalay, O., Suter, U., Machado, R.A.C., Roccio, M., Lutolf, M.P., Semenkovich, C.F. and Jessberger, S., 2013. Metabolic control of adult neural stem cell activity by Fasn-dependent lipogenesis. *Nature*, **493**: 226-230. <https://doi.org/10.1038/nature11689>
- Leonard, J.V. and Schapira, A.H., 2000. Mitochondrial respiratory chain disorders I: mitochondrial DNA defects. *Lancet*, **355**: 299-304. [https://doi.org/10.1016/S0140-6736\(00\)78142-8](https://doi.org/10.1016/S0140-6736(00)78142-8)



- [org/10.1016/S0140-6736\(99\)05225-3](https://doi.org/10.1016/S0140-6736(99)05225-3)
- Lepesheva, G.I. and Waterman, M.R., 2011. Structural basis for conservation in the CYP51 family. *Biochim. biophys. Acta*, **1814**: 88-93. <https://doi.org/10.1016/j.bbapap.2010.06.006>
- Liu, Z.H. and Huang, X., 2013. Lipid metabolism in Drosophila: development and disease. *Acta Biochim. Biophys. Sin.*, **45**: 44-50. <https://doi.org/10.1093/abbs/gms105>
- Luoma, A.M., Kuo, F., Cakici, O., Crowther, M.N., Denninger, A.R., Avila, R.L., Brites, P. and Kirschner, D.A., 2015. Plasmalogen phospholipids protect internodal myelin from oxidative damage. *Free Radic. Biol. Med.*, **84**: 296-310. <https://doi.org/10.1016/j.freeradbiomed.2015.03.012>
- Ma, S., Sun, S.H., Geng, L.L., Song, M.S., Wang, W., Ye, Y.X., Ji, Q.Z., Zou, Z.R., Wang, S., He, X.J., Li, W., Esteban, C.R., Long, X., Guo, G.J., Chan, P., Zhou, Q., Belmonte, J.C.I., Zhang, W.Q., Qu, J. and Liu, G.H., 2020. Caloric restriction reprograms the single-cell transcriptional landscape of rattus norvegicus aging. *Cell*, **180**: 984-1001. <https://doi.org/10.1016/j.cell.2020.02.008>
- Madiraju, A.K., Erion, D.M., Rahimi, Y., Zhang, X.M., Braddock, D.T., Albright, R.A., Prigaro, B.J., Wood, J.L., Bhanot, S., MacDonald, M.J., Jurczak, M.J., Camporez, J.P., Lee, H.Y., Cline, G.W., Samuel, V.T., Kibbey, R.G. and Shulman, G.I., 2014. Metformin suppresses gluconeogenesis by inhibiting mitochondrial glycerophosphate dehydrogenase. *Nature*, **510**: 542-546. <https://doi.org/10.1038/nature13270>
- Mao, X.Z., Cai, T., Olyarchuk, J.G. and Wei, L.P., 2005. Automated genome annotation and pathway identification using the KEGG Orthology (KO) as a controlled vocabulary. *Bioinformatics*, **21**: 3787-3793. <https://doi.org/10.1093/bioinformatics/bti430>
- Marcher, A.B., Loft, A., Nielsen, R., Vihervaara, T., Madsen, J.G.S., Sysi-Aho, M., Ekroos, K. and Mandrup, S., 2015. RNA-Seq and mass-spectrometry-based lipidomics reveal extensive changes of glycerolipid pathways in brown adipose tissue in response to cold. *Cell Rep.*, **13**: 2000-2013. <https://doi.org/10.1016/j.celrep.2015.10.069>
- Mei, L., Zhang, H., Zhu, W.L. and Wang, Z.K., 2019. Seasonal variations of adipose tissue in *Tupaia belangeri* (Mammalia: Scandentia: Tupaiidae). *Eur. Zool. J.*, **86**: 54-62. <https://doi.org/10.1080/24750263.2019.1572798>
- Moon, Y.A. and Horton, J.D., 2003. Identification of two mammalian reductases involved in the two-carbon fatty acyl elongation cascade. *J. Biol. Chem.*, **278**: 7335-7343. <https://doi.org/10.1074/jbc.M211684200>
- Nagao, K., Murakami, A. and Umeda, M., 2019. Structure and function of delta 9-fatty acid desaturase. *Chem. Pharm. Bull.*, **67**: 327-332. <https://doi.org/10.1248/cpb.c18-01001>
- Orr, A.L., Ashok, D., Sarantos, M.R., Ng, R., Shi, T., Gerencser, A.A., Hughes, R.E. and Brand, M.D., 2014. Novel inhibitors of mitochondrial sn-glycerol 3-phosphate dehydrogenase. *PLoS One*, **9**: e89938. <https://doi.org/10.1371/journal.pone.0089938>
- Peltoketo, H., Luu-The, V., Simard, J. and Adamski, J., 1999. 17 beta-hydroxysteroid dehydrogenase (HSD) /17-ketosteroid reductase (KSR) family; nomenclature and main characteristics of the 17HSD/KSR enzymes. *J. mol. Endocrinol.*, **23**: 1-11. <https://doi.org/10.1677/jme.0.0230001>
- Rosell, M., Kaforou, M., Frontini, A., Okolo, A., Chan, Y.W., Nikolopoulou, E., Millership, S., Fenech, M.E., MacIntyre, D., Turner, J.O., Moore, J.D., Blackburn, E., Gullick, W.J., Cinti, S., Montana, G., Parker, M.G. and Christian, M., 2014. Brown and white adipose tissues: Intrinsic differences in gene expression and response to cold exposure in mice. *Am. J. Physiol. Endocrinol. Metab.*, **306**: E945-E964. <https://doi.org/10.1152/ajpendo.00473.2013>
- Schoepp, B., Breton, J., Parot, P. and Vermeglio, A., 2000. Relative orientation of the hemes of the Cytochrome *bc*<sub>1</sub> complexes from *Rhodobacter sphaeroides*, *Rhodospirillum rubrum*, and beef heart mitochondria: A linear dichroism study. *J. Biol. Chem.*, **275**: 5284-5290. <https://doi.org/10.1074/jbc.275.8.5284>
- Shore, A.M., Karamitri, A., Kemp, P., Speakman, J.R., Graham, N.S. and Lomax, M.A., 2013. Cold-induced changes in gene expression in brown adipose tissue, white adipose tissue and liver. *PLoS One*, **8**: e68933. <https://doi.org/10.1371/journal.pone.0068933>
- Sunaga, H., Matsui, H., Ueno, M., Maeno, T., Iso, T., Syamsunarno, M.R.A.A., Anjo, S., Matsuzaka, T., Shimano, H., Yokoyama, T. and Kurabayashi, M., 2013. Deranged fatty acid composition causes pulmonary fibrosis in *Elovl6*-deficient mice. *Nat. Commun.*, **4**: 2563. <https://doi.org/10.1038/ncomms3563>
- Traurig, M.T., Orczewska, J.I., Ortiz, D.J., Bian, L., Marinellarena, A.M., Kobes, S., Malhotra, A., Hanson, R.L., Mason, C.C., Knowler, W.C., Bogardus, C. and Baier, L.J., 2013. Evidence for

- a role of *LPGATI* in influencing BMI and percent body fat in Native Americans. *Obesity*, **21**: 193-202. <https://doi.org/10.1002/oby.20243>
- Wang, D.H. and Wang, Z.W. 1990. Strategies for survival of small mammals in a cold alpine environment II-seasonal changes in the capacity of no shivering thermogenesis in *Ochotona curzoniae* and *Microtus oeconomus*. *Acta Theriol. Sin.*, **10**: 40-53.
- Wang, H.N., Chen, H.D., Chen, K.Y., Xiao, J.F., He, K., Xiang, G.A. and Xie, X., 2013. Highly expressed MT-ND3 positively associated with histological severity of hepatic steatosis. *Acta Pathol. Microbiol. Immunol. Scand.*, **122**: 443-451. <https://doi.org/10.1111/apm.12166>
- Watanabe, M., Yamamoto, T., Yamamoto, A., Obana, E., Niiyama, K., Hada, T., Ooie, T., Kataoka, M., Hori, T., Houchi, H. and Shinohara, Y., 2011. Differential effects of cold exposure on gene expression profiles in white versus brown adipose tissue. *Appl. Biochem. Biotechnol.*, **165**: 538-547. <https://doi.org/10.1007/s12010-011-9273-4>
- Zhang, L., Yang, F., Wang, Z.K. and Zhu, W.L., 2017. Role of thermal physiology and bioenergetics on adaptation in tree shrew (*Tupaia belangeri*): The experiment test. *Sci. Rep.*, **49**: 740-753. <https://doi.org/10.1038/srep41352>
- Zhu, M.M., Xie, R.Q., Chen, L.Y., You, M.H., Gou, W.L., Chen, C., Li, P. and Cai, Y.M., 2021. Milk production and quality of lactating yak fed oat silage prepared with a low-temperature-tolerant lactic acid bacteria inoculant. *Foods*, **10**: 2437. <https://doi.org/10.3390/foods10102437>

Online First Article